Quasi-parabolic reflecting bottom surfaces of the Drygalski Antarctic floating ice tongue

Cesidio Bianchi ([1]), **Massimo Chiappini** ([1]), **Ignazio E. Tabacco** ([2]), **Achille Zirizzotti** ([1]) **and Enrico Zuccheretti** ([1])

([1]) *Istituto Nazionale di Geofisica e Vulcanologia, Roma, Italy*

([2]) *Università di Milano, Sezione Geofisica, Milano, Italy*

Abstract

Very high frequency deep radio sounding systems for ice thickness measurements are practically the only useful apparatuses for large scale radar flight surveys in polar regions. The morphology of the bottom surface of an Antarctic floating ice tongue, in the Ross Sea area, East Antarctica, was studied using the arrival times of signal echoes of the radio sounding system. The amplitude variations of radar signals from the reflecting surface were analyzed to determine the gain or the loss of the reflectors. Such surfaces show quasi-parabolic geometrical shapes at the ice/water interface with both concave and convex faces towards the sounding system. Electromagnetic analysis performed on radar echoes indicates that amplitude variations detected by the antenna are focusing or defocusing effects only due to the reflector's shape. A factor in the radar equation that represents the surface shape when coherent reflectors are involved is introduced. This factor allows us to determine more precisely the morphology and electromagnetic characteristics of the interface between the media investigated by means of radio echo sounding.

Key words *radio echo sounding – radio glaciology – glacier ice tongues*

1. Introduction

Floating ice tongues are interesting to evaluate the electromagnetic properties of the media involved in radar sounding. Among the floating ice tongues, the Drygalski Glacier is interesting because of its bottom morphology and ice thickness. Figure 1 shows the location of the Drygalski Glacier ice tongue.

A longitudinal profile of the bottom surface, surveyed at an elevation of about 300 m from the ice surface, showed a rippled bottom morphology with a shape of rather regular waves with a spatial length of about 1-2 km, and with a depth variation of hundreds of meters (Tabacco *et al.*, 2000). The analyzed ice thickness ranging between 150-500 m was calculated assuming a radio wave velocity of 168 m/μs (Bogorodsky *et al.*, 1985).

Figure 2 represents a sounding profile of the ice tongue with the rippled bottom surface. The profile was obtained maintaining the airborne radio echo sounding system at a nearly constant terrain clearance with a horizontal sampling rate of about 20 traces/km.

A single radar trace in shown in fig. 3; all traces along the surveyed glacier profile furnish a quantitative evaluation of the signal amplitude along the whole horizontal profile.

After a brief description of the airborne acquisition and sounding system, the electromag-

Mailing address: Dr. Cesidio Bianchi, Istituto Nazionale di Geofisica e Vulcanologia, Via di Vigna Murata 605, 00143 Roma, Italy; e-mail: bianchi@ingv.it

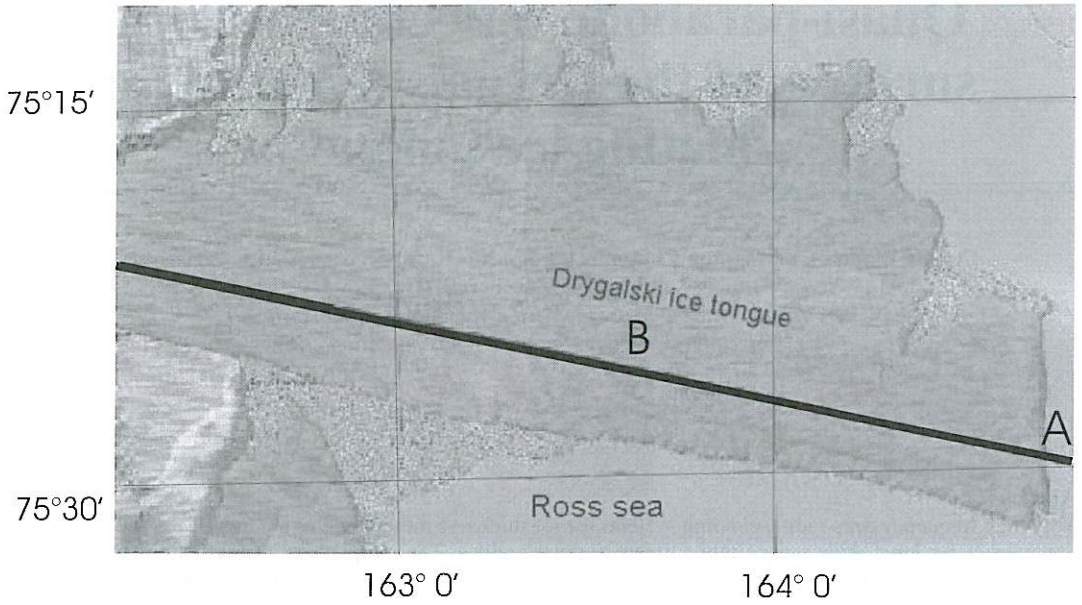

Fig. 1. David-Drygalski glacier: USGS topographic map with the survey flight. Letters A and B indicate the beginning and the end of the examined profile.

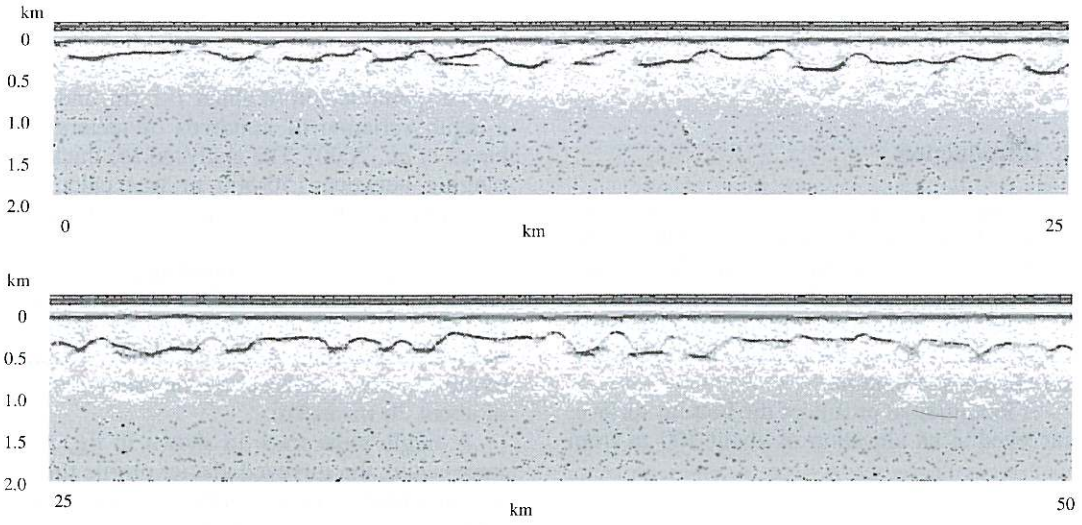

Fig. 2. Ice thickness *versus* distance of Drygalski ice glacier is reported: a profile of about 50 km is divided into two parts.

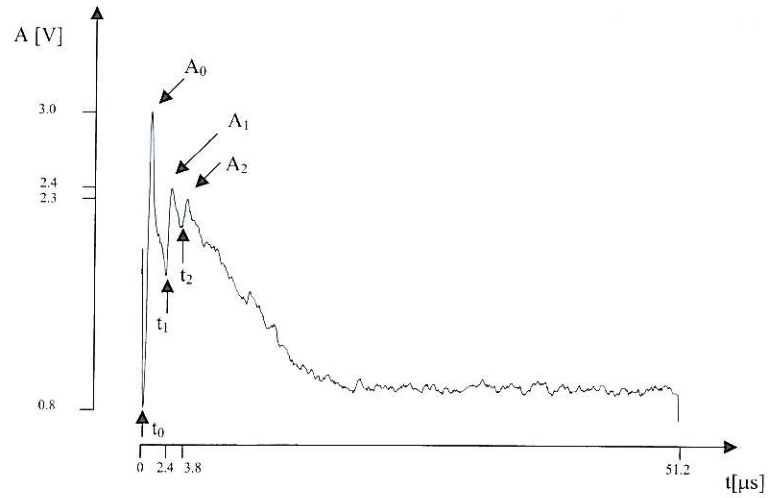

Fig. 3. Examples of radar trace: on the *x*-axis the 51.2 μs listening time is indicated as well as relevant arrival times, while on the *y*-axis the relative amplitude of the signal in a voltage scale is shown.

netic approach and data processing are presented. The correlation between signal amplitude and bottom reflection surfaces is discussed.

2. System characteristics and calibration

The employed airborne radio sounding system operates at 60 MHz with a pulse length 0.3-1 μs and a transmitted power of about 62 dBm (Tabacco *et al.*, 1999). The employed wavelength does not allow sophisticated antenna geometry and the radar employed uses dipole or other linear antennas arranged beneath the wings of a small aircraft.

Navigation relied upon a GPS receiver on board giving longitude, latitude, altitude and time for each acquired radar trace.

The 51.2 μs time duration of the received analog echo signal was digitized at the sampling frequency of 20 MHz. Previous laboratory tests on the 16 MHz bandwidth log-receiver furnished a range resolution of 8 m which includes digitizing errors even in case of poor signal-to-noise ratio up to 3 dB.

The large receiver bandwidth allows us to neglect the receiver saturation due to the transmitted pulse, antenna ringing and the first strong incoming echo, as well as high bias level due to the strongest echoes when the lower levels of amplitude are scaled (Tabacco *et al.*, 2000).

The relation between the input and the output of the log-receiver is the following:

$$V_i = 10^{\frac{V_0 - 3.7}{0.5}} \qquad (2.1)$$

where, V_0, V_i are the amplitudes, expressed in volts, of the output and input signals of the receiver, respectively.

Relation (2.1) is valid only in the receiver sensitivity range, from – 110 dBm to – 20 dBm.

The well known expression describing the received signal power available at the input of the receiver P_r related to the transmitted power P_t:

$$P_r = P_t \lambda^2 G^2 / (4\pi D)^2 R \qquad (2.2)$$

was used for calibration. D is the distance covered along the propagation path, G is the antenna gain; λ the wavelength, and R represents the reflection loss *i.e.* the power loss at the air/ice and air/seawater interfaces, calculated from the relative dielectric permittivity reported in table I.

Table I. Electromagnetic properties of the considered media.

Medium	Relative permittivity $\varepsilon r'$	Conductivity σ [S/m]
Air	1.0	0
Ice	3.18	$7.95 \cdot 10^{-6}$
Seawater	84.4	4
Sea ice	3.44	$10^{-2} - 10^{-1}$

System calibration was performed in two different reflecting flat surfaces (ice and water), to evaluate the contribution of the G term assuming the same gain, for both transmitting and receiving antennas. P_t, D, R are known quantities, whereas P_r is deduced using relation (2.1) from the received signal amplitude measured at the receiver output.

Test flights at increasing altitude and different receiver gain were performed to operate with several levels of received signal avoiding problems due to the saturation of the logarithmic receiver and it was found that $G \cong 2.5$ dB. The calibration of the sounding system showed the same result, when operating on both air/ice and air/seawater interfaces.

3. Amplitude analysis

The echo signal containing information of all the losses and gains of the radio wave along its propagation path was analyzed to evaluate the variation of the received echo signals in detail.

Assuming the electromagnetic properties of ice constant in the whole ice tongue, it is possible to determine the radio electric power of the echo signal from relation (2.2) which can be expressed in dB as follows:

$$P_r = P_t + G - L \pm S \quad [\text{dB}] \qquad (3.1)$$

where L is the total loss given by several contributions: absorption of the medium, reflection and transmission losses at the interface between the media, and the geometric loss. The term S, representing the gain-loss factor related to the reflector shape (the bottom morphology, in our case), is the unknown quantity to be calculated.

The gain due the refractive effect of ice (existing in case of flat surface as well) can be neglected for small ice thicknesses. It depends on the air to ice dielectric permittivities ratio and the terrain clearance to ice thickness ratio (Bogorodsky). We foresee that the concave and convex faces of the ice/seawater interface reflector cause a focusing or defocusing effect in the echo signal producing a high amplitude variation. Such a contribution observed in the received amplitude can be evaluated only if the total propagation loss L is fully known.

In this electromagnetic analysis, it is reasonable to assume that the transmission and the reflection coefficients do not change along the horizontal profile. Therefore, considering all the loss contributions, L can be expressed as

$$L = L_D + L_a + L_R + L_T + L_p + L_s \quad [\text{dB}] \qquad (3.2)$$

where L_D is the geometrical loss due to the distance of the reflector, L_a is the absorption of the ice, L_R and L_T are the reflection and the transmission losses at the interface (table II), L_p is the polarization loss due to the orientation of the receiving antenna with respect to the received radio wave and L_s is the scattering loss.

Considering the temperature of ice constant for the whole surveyed profile as well as chemical composition and surface roughness, the electromagnetic properties can be calculated (*e.g.*, as in Frolik and Yagle, 1995; Herique and Kofman, 1997) throughout the length of the profile (table I).

Table II. Percentage of power lost through the interfaces considered; R and T are the reflection and transmission coefficients.

Interface	Reflected power ratio R^2	Transmitted power ratio $T^2 = 1 - R^2$
Air/ice ice/air	0.08	0.92
Air/seawater	0.64	0.36
Ice/seawater	0.61	0.39
Ice/sea ice	$4 \cdot 10^{-4}$	0.9996

The acquired radar trace as in fig. 3 allows us to scale the time values to calculate the geometric loss L_D and the attenuation loss L_a. The geometrical attenuation including the factor $\left(\frac{\lambda}{4\pi}\right)^2$ is given by

$$L_D = 20 \cdot \mathrm{Log} \frac{D \cdot 4\pi}{\lambda} \qquad (3.3)$$

where $D = 168 \cdot 2 \cdot t$ being t the delay time of the considered reflector as in fig. 3.

If we assume the conductivity σ in the ice as reported in table I, L_a can be evaluated as

$$L_a = \mathrm{const} \cdot \sigma \cdot d \qquad (3.4)$$

being $d = 168 \cdot 2 \cdot (t_2 - t_1)$ *i.e.* twice the ice thickness.

In the following analysis L_p and L_s have been neglected because of their small contribution (less than 0.5 dB).

The dielectric permittivity of the various media also allows us to calculate the reflection

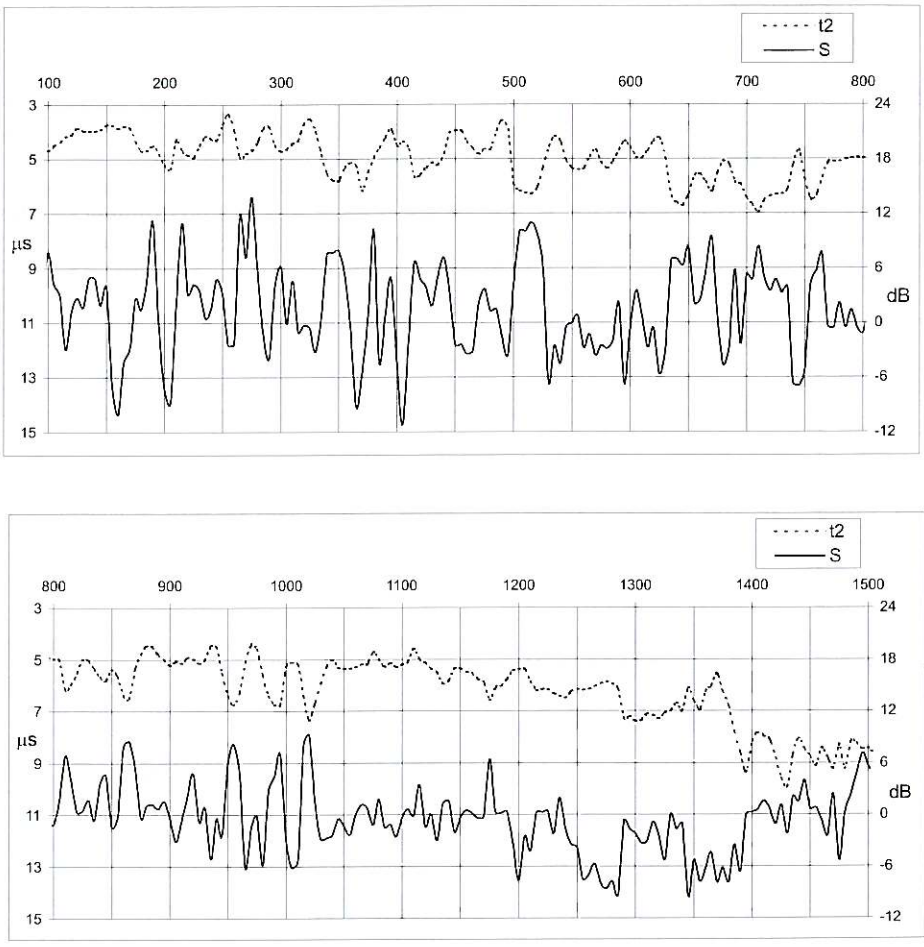

Fig. 4. Smoothed bottom surface profile (distance *versus* ice thickness variation) and relative amplitude variation in dB.

and the transmission percentage of power losses R^2 and T^2 respectively (table II). The total contribution of the reflection and transmission losses is about 5dB.

The received signal power at the antenna input P_r is obtained using the relation (2.1) from the voltage amplitude measured at the receiver output.

Adding all the contributions of (3.1) and combining with (3.2), S can be finally evaluated as

$$S = P_r - P_t - G + L_D + L_a + L_R + L_f \text{ [dB]}. \quad (3.5)$$

In theory, for flat reflectors, homogeneous ice, and a perfect calibration, relation (3.5) is reduced to $S = 0$. On the other hand, non flat reflectors would produce positive or negative values of S following the geometrical shape at the ice/seawater interface. A relatively high positive value for S is expected when there is a concave parabolic-like reflecting surface (focusing effect), while a convex surface is assumed to give a negative contribution.

In fig. 4, there is an evident relation between S values and bottom reflection surface shape (curve t_2). The two plotted lines show nearly the same variation with opposite phase. Concave surfaces produce very strong signal amplitudes while convex surfaces give negative contributions.

Correlation and spectral analyses were performed on bottom reflection surface and signal data sets. The relatively large Pearson's correlation coefficient (0.75) and the remarkable coincidence between the frequency spectra of both series (fig. 5) confirm the focusing or defocusing effects detected by the system and the relation existing between the S function and the bottom shape.

We performed a numerical simulation aimed at the modeling of the sub-ice features to explain amplitude variations found during the measurements.

The bottom reflecting surfaces shown in fig. 2 were divided into different segments corresponding to concave and convex faces and

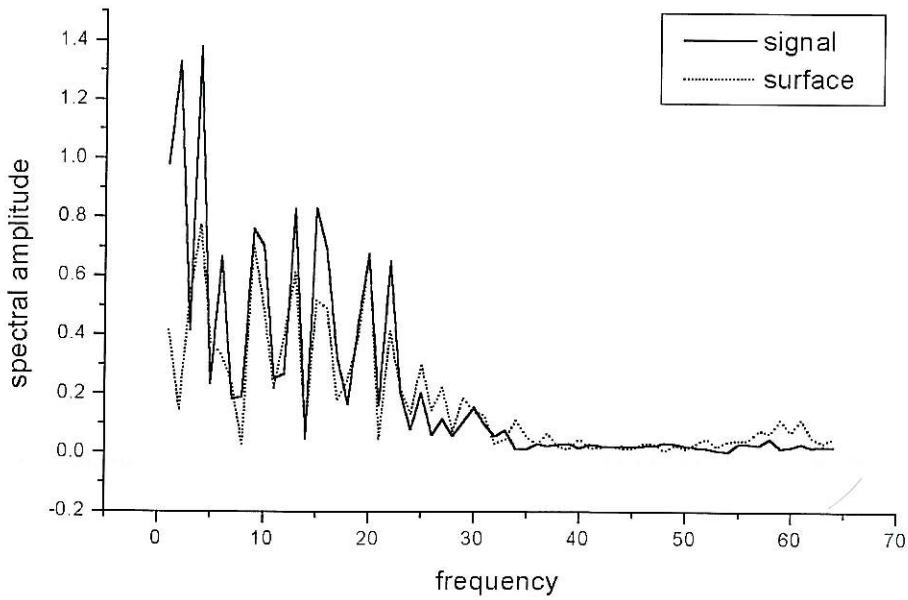

Fig. 5. Spectral amplitude *versus* frequency of the ice thickness (dashed line) and amplitude variation of the signal (solid line), in arbitrary units. The harmonic components, except the one at the lowest frequency, have the same values.

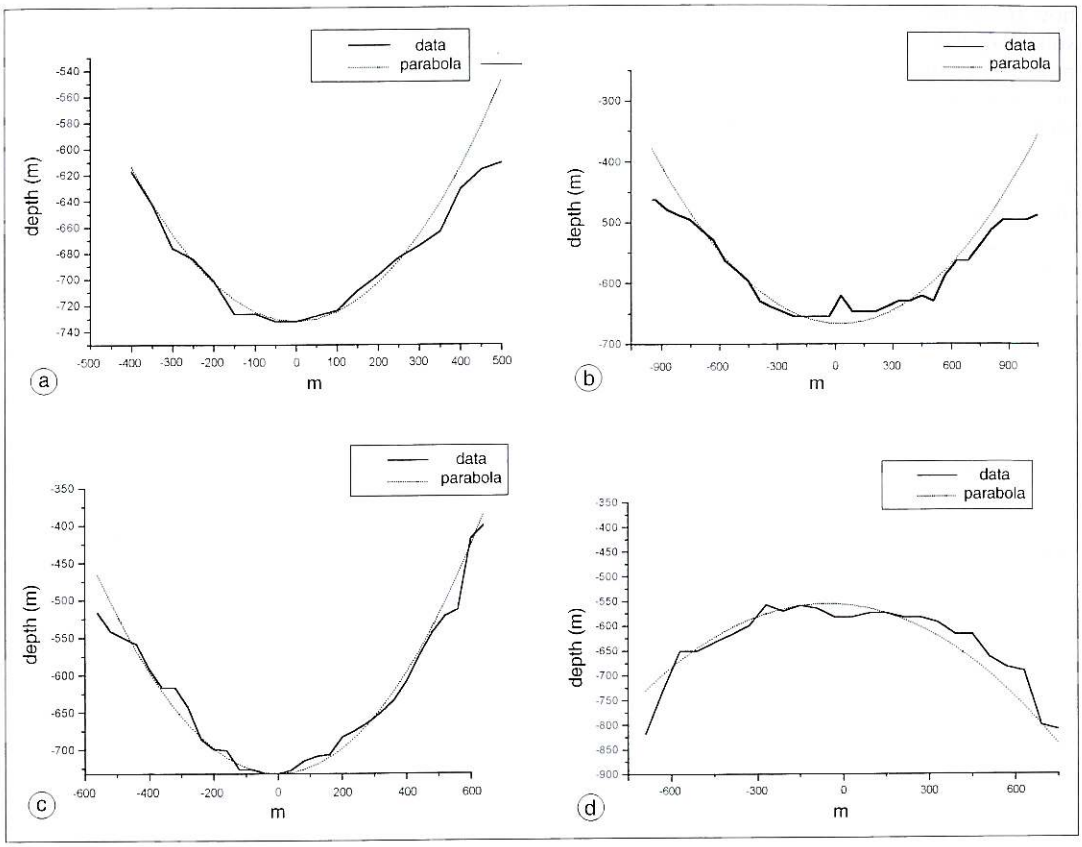

Fig. 6a-d. The quadratic regression shows that the parabolas approximated the concave reflectors when they are in correspondence with the highest level of recorded signal amplitude (a-c) and convex reflector in correspondence with the lowest level of the signal (d).

the single reflectors were studied. Four particular concave reflectors corresponding to the highest and lowest levels of recorded signal amplitude were analyzed (fig. 6a-d). The curve that best fits the selected sectors of the profile is a parabola whose vertex is at the minima of the curve t_2.

Positioning the origin of the reference system coinciding with the flight altitude, the parabola vertex is nearly in correspondence with the minimum of the considered data set (fig. 6a-c). The resulting position of the parabola focus is very close to the flight altitude.

When concavity is towards the sounding system, a focusing gain around 8 dB is expected. A signal attenuation of 8 dB is found when the parabola shows the convex face to the antenna system as shown in fig. 6d.

4. Conclusions

When performing airborne radio echo surveys, the observed signal amplitudes may be affected by focusing or defocusing effects due to the particular shape of sub-ice reflectors. In the present paper we have shown an example of

how these effects can be estimated. Radio echo sounding data carried out along a longitudinal profile over the Drygalski ice tongue in Antarctica were used to develop an electromagnetic analysis which has shown a correspondence between the shape of the bottom reflecting surface (ice/seawater interface) and the signal amplitude. Amplitude variations of ± 8 dB are well explained with a quasi-parabolic reflector that exhibits concave or convex face towards the sounding apparatus.

Acknowledgements

The authors wish to thank Mrs. Silvia Pau for careful preparation of the figures in the present paper as well as article format. The useful criticism of Dr. Giovanni Romeo is greatly appreciated.

REFERENCES

BOGORODSKY, V.V., C.R. BENTLEY and P.E. GUDMANDSEN (1985): *Radioglaciology* (Reidel Publ. Company), pp. 254.

FROLIK, J.L and A.E. YAGLE (1995): Reconstruction of multilayered lossy dielectric from plane wave impulse response at two angle of incidence, *IEEE Trans. Geosci. Remote Sensing*, **33** (2), 268-279.

HERIQUE, A. and W. KOFMAN (1997): Determination of the ice dielectric permittivity using the data of the test in Antarctica of the ground-penetrating radar for Mars '98, *IEEE Trans. Geosci. Remote Sensing*, **35** (2), 1338-1349.

TABACCO, I.E., C. BIANCHI, M. CHIAPPINI, A. PASSERINI, A. ZIRIZZOTTI and E. ZUCCHERETTI (1999): Latest improvements for the echo sounding system of the Italian radar glaciological group and measurements in Antarctica, *Ann. Geofis.*, **42** (2), 271-276.

TABACCO, I.E., C. BIANCHI, M. CHIAPPINI, A. ZIRIZZOTTI and E. ZUCCHERETTI (2000): Analysis of the bottom topography of the glacier ice tongue of Ross Sea Coast Line (Antarctica), *Ann. Glaciology*, **30**, 47-51.

(received February 12, 2001;
accepted April 4, 2001)